Journal of Magnetism and Magnetic Materials 349 (2014) 95–99

Contents lists available at ScienceDirect

Journal of Magnetism and Magnetic Materials

journal homepage: www.elsevier.com/locate/jmmm

Analytical comparison of magnetic and electrical properties using modified Landau theory in bismuth ferrite: Effect of milling

Pardeep K. Jha [a,*], Priyanka A. Jha [a,b], Geetika Srivastava [a], A.K. Jha [b,c], R.K. Kotnala [d], R.K. Dwivedi [a]

[a] Department of Physics and Materials Science & Engineering, Jaypee Institute of Information Technology, Noida, UP 201307, India
[b] Thin Film & Material Science Laboratory Department of Applied Physics, Delhi Technological University (Formerly Delhi College of Engineering) Bawana Road, Delhi 110042, India
[c] Department of Applied Sciences, A.I.A.C.T.R. Geeta Colony, Delhi 110031, India
[d] National Physics Laboratory, Dr. K.S. Krishanan Marg, New Delhi 110012, India

ARTICLE INFO

Article history:
Received 13 March 2013
Received in revised form
19 August 2013
Available online 27 August 2013

Keywords:
Multiferroic
Bismuth ferrite
Mechanochemical activation technique

ABSTRACT

In this study, authors have synthesized bismuth ferrite using (i) solid state route and (ii) mechanochemical activation technique. The structural studies reveal the formation of bismuth ferrite of $A_{3-\delta}B_5O_{12}$ type by mechanochemical activation technique and of ABO_3 type by conventional solid state route. In addition to the detailed studies on magnetic and electrical properties of both the samples, a comparative analysis has been done using Landau and Berry phase theory. Through this, an effort has been made to establish a relationship between magnetism and electrical polarization vis a vis magneto-electric coupling in these samples.

1. Introduction

$BiFeO_3$ (BFO) is a well known multiferroic material which shows ferroelectric and anti-ferromagnetic coupling at room temperature. It has already been recognized that the suppression of helical order existing with a periodicity of 62 nm on canted anti-ferromagnetic order between two successive (111) ferromagnetic planes might give rise to higher magnetization. The decrease in particle size below the periodicity of the helical order will lead to the suppression of the antiferromagnetically ordered spin cycloid [1]. This prompted the authors to increase the magnetization by reducing the particle size. Hence, an attempt has been made to synthesize nano-structured bismuth ferrite using high-energy planetary ball milling (HEPBM) which usually results in large density of crystal defects in the final samples. This, in turn, can lead to unexpected magnetic properties of the nano-structured materials [2]. As Bi is volatile and the thermodynamics in HEPBM led to the formation of $Bi_{3-\delta}Fe_5O_{12}$ (off stoichiometric bismuth iron garnet (BIG)). The result is not very surprising as some X-ray diffraction (XRD) peaks similar to this have also been reported by Ref. [3], though they had identified it as an impurity in BFO. BIG preparation many times results in impurity phases of BFO and vice versa [4,5]. The formation of BIG in HEPBM process inspired the authors to study the mechanism of formation and the role of HEPBM in inducing defects in the sample. In this work, a comparative study of the magnetic and electrical properties of the samples prepared by conventional solid state route and by HEPBM has been reported. The thermodynamics of the phase transition was described by Landau [6]. Landau theory was first used by Devonshire for ferroelectric materials [7] and then modified by Ginzberg for unpoled bulk ferroelectrics [8,9]. Finally, for multiferroic materials modifications were reported by Ref. [10]. Hence a thermodynamic analysis has been carried out in order to justify the formation of BIG by mechanochemical activation technique with the help of Landau theory. The free energy has been analyzed through the thermodynamics lying behind the hysteresis curves.

2. Experimental

Highly pure powders of Bi_2O_3 and Fe_2O_3 (Sigma Aldrich) were mixed in stoichiometric (with 5 mol.% extra Bi_2O_3) proportions to form $BiFeO_3$ by two synthesizing routes. First by conventional solid state route (SSR), in which the precursors were calcined at 700 °C for 1 h after grinding. In second route, mechanochemical treatment was performed in a planetary ball mill (Retsch PM100) with milling speed 400 rpm. Milling was carried out in toluene medium with high wear resistant 10 mm steel balls in a steel vial for effective 40 h. The milling vessels were stopped for 30 min after each hour of milling for removing the water vapor overpressure,

* Corresponding author. Tel.: +91 9654316768; fax: +91 120 2 40 09 86.
E-mail address: pardeepjha.jiit@gmail.com (P.K. Jha).

0304-8853/$ - see front matter © 2013 Elsevier B.V. All rights reserved.
http://dx.doi.org/10.1016/j.jmmm.2013.08.048

since the temperature of the vessel rises during the milling process. The mixtures obtained by two methods were then admixed with PVA as a binder and then pressed at 100 MPa into disk shaped pellets using co-axial hydraulic press. These pellets were then sintered at 830 °C for 2 h in air on alumina disk. Phase development in the calcined powder, mechanically activated powder and sintered pellets were monitored using X-ray diffractometer (Bruker, D8 advance) with CuKα radiation ($\lambda = 1.5405$ Å) with scanning rate of 1°/min. Scanning electron microscopy (Hitachi, S3700) was used to study surface morphology of sintered pellets. The sintered pellets were polished and coated with silver paste on both sides and cured at 325 °C for half an hour. Magnetic measurements at room temperature (M–H loop) have been carried out using Vibrating Sample Magnetometer (VSM 7305, Lake Shore). P–E loops have been traced using Sawyer-Tower circuit. Dielectric studies have been carried out using Novocontrol Alpha-AT Impedance Analyser. Magneto-electric coupling coefficient has been deduced as described in [11].

XRD patterns were analyzed using least square refinement method by the computer program package Powder X [12]. SEM images were analyzed using ImageJ software. Average areal Grain size has been calculated from band pass filtered SEM images, using Jeffries' grain counting method (section 9, E112-96) with the help of ImageJ.

3. Results and discussions

3.1. Structural analysis

Fig. 1(a) shows the X-ray diffraction patterns of the sample synthesized using SSR and mechanochemically activated sample (milled for 40 h) sintered at 830 °C (abbreviated as A1 and N40 respectively). It is observed that the phase of A1 is of BFO, while the phase of N40 is closely matching with $Bi_{2.46}Fe_5O_{12}$ in accordance with the JCPDS File (No. 01-086-0367). A careful analysis has been done in order to identify the secondary phases in the XRD pattern, secondary phases observed are $Bi_2Fe_4O_9$, Fe_3O_4 as indicated in Fig. 1(a). The lattice parameters were calculated with the observed d-values. The structure of A1 is Rhombohedral with R3c symmetry ($a = 13.3362$ Å, $c = 5.6262$ Å) whereas the structure of N40 sample is cubic with $I4_1/a$ symmetry ($a = 12.6360$ Å). The surface morphology of N40 (nano-materials) is different from A1 (bulk-materials) due to their grain size as seen in the SEM micrographs Fig. 1(b). Thermodynamics of nucleation plays an important role as it decides the shape and size of the grain. The areal grain size of the N40 (3.20 μm^2) is very small in comparison to A1 (1067.43 μm^2), resulting in higher surface energy and hence different properties. Hence Gibbs free energy for the formation of nano-size grain is much higher than the bulk. For the stable grain formation, Gibbs free energy has to be minimized and for the milled sample, it can be attained by losing some atoms from the regular lattice sites which creates the defects in the sample, especially at the interfaces [13].

It is well known that during milling, acceleration between the balls is too large even more than acceleration due to gravity at earth's surface [2]. Thus, a huge amount of energy is generated in ball-milling and this might have led to the formation of BIG (N40) instead of BFO (A1). Moreover, the bond dissociation energy and enthalpy of formation of various bonds [14] suggest the formation of charge carriers in A1 and N40 (ignoring secondary phases), as depicted in the following equations:

$$1.05(Bi_2O_3) + Fe_2O_3 \rightarrow 2BiFeO_3 + 0.05(2Bi\uparrow + 2V_{Bi}^{'''}) + 0.075(O_2\uparrow + 2V_O^{\bullet\bullet}) \quad (1)$$

$$1.05(Bi_2O_3) + Fe_2O_3 \rightarrow 0.4Bi_{2.46}Fe_5O_{12} + 0.558(2Bi\uparrow + 2V_{Bi}^{'''}) + 0.675(O_2\uparrow + 2V_O^{\bullet\bullet}) \quad (2)$$

From the above defect equations, on comparing the concentration of vacancy formation, it has been found that the formation of

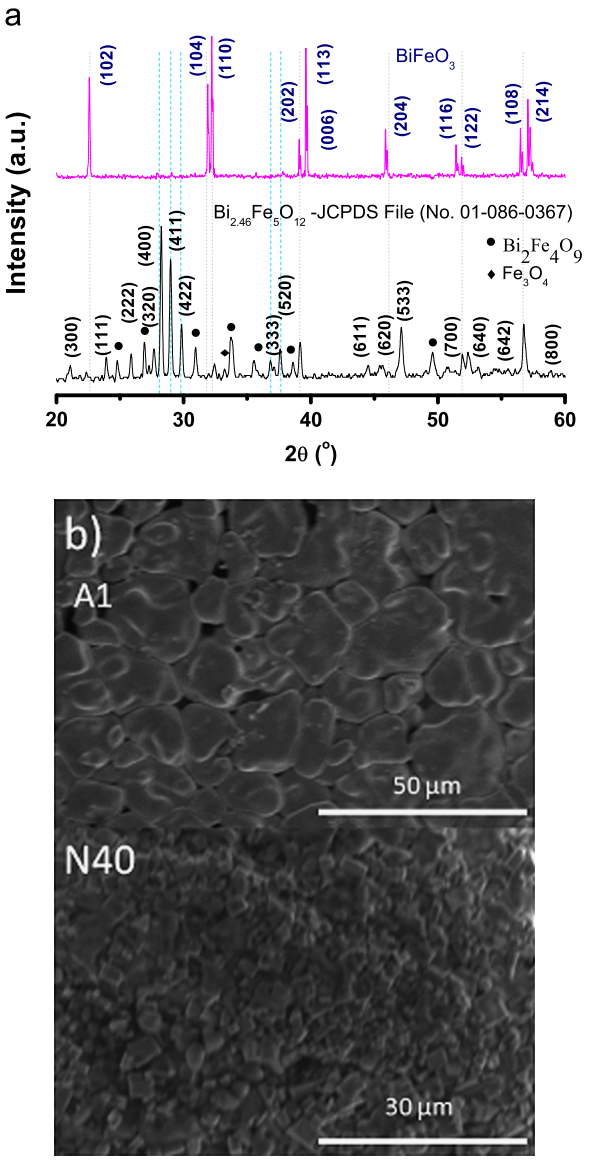

Fig. 1. Comparison of (a) XRD and (b) SEM images of BFO (A1) and BIG (N40) samples. (For interpretation of the references to color in this figure caption, the reader is referred to the web version of this paper.)

Bismuth vacancies are 11.16 (=0.558/0.05) times more in N40 than A1 whereas the formation of oxygen vacancies is 9 (=0.675/0.075) times more in N40 than A1 for same amount of precursors. Further molar ratio of formation of BFO to BIG is 5 (=2 × 1/0.4) for given amount of precursors. It means bismuth vacancies are 5 × 11.16= 55.88 and oxygen vacancies are 5 × 9=45 times more for one formula unit of N40 as compared to A1.

3.2. Magnetic hysteresis analysis

The M-H measurements for A1 and N40 (Fig. 2(a)) indicate antiferromagnetic behavior for A1 [15], while the ferrimagnetic behavior for N40. The area of magnetic hysteresis loops estimates the energy losses. Hence, the free energy (Δg) associated with two hysteresis curves has been plotted with magnetic field (H) (dashed line in Fig. 2(a)) and magnetic moment/g (M) (in Fig. 2(b)). It is expanded (as [7]) polynomially up to sixth power of M (fitted